Journal of Petroleum Science and Engineering 68 (2009) 60–70

Contents lists available at ScienceDirect

Journal of Petroleum Science and Engineering

journal homepage: www.elsevier.com/locate/petrol

Well-data-based prediction of productivity decline due to sulphate scaling

Pavel Bedrikovetsky [a,*], Raphael M.P. Silva [b], José S. Daher [c], José A.T. Gomes [c], Vera C. Amorim [c]

[a] University of Adelaide, Australian School of Petroleum, Adelaide SA5005, Australia
[b] North Fluminense State University — UENF, Laboratory of Petroleum Engineering and Exploration — LENEP Rua Sebastiao Lopes da Silva, 56. Riviera Fluminense, Macaé, 27937-560, RJ, Brazil
[c] PETROBRAS/UNBC, Avenida Elias Agostinho 665 CEP 27913-350 Imbetiba, Macae, RJ, Brazil

ARTICLE INFO

Article history:
Received 9 December 2006
Accepted 7 June 2009

Keywords:
reactive flow
porous media
sulphate
scaling
productivity index
formation damage

ABSTRACT

Sulphate scaling can have a disastrous impact on oil production in waterflood projects with incompatible injected and formation waters. This is due to precipitation of barium/strontium sulphate from the mixture of both waters and the consequent permeability reduction resulting in loss of well productivity.

The system where sulphate scaling damage occurs is determined by two governing parameters: the kinetics coefficient characterising the velocity of chemical reaction and the formation damage coefficient reflecting permeability decrease due to salt precipitation.

Previous work has derived an analytical model-based method for determination of two coefficients from laboratory corefloods during quasi-steady state commingled flow of injected and formation waters. The current study extends the method for determination of kinetics and formation damage coefficients from production well data consisting of barium concentrations in the produced water and of well productivity decline.

We analyse production data for five wells from giant offshore field A, submitted to seawater flooding (Campos Basin, Brazil), and obtain values of the two sulphate scaling damage parameters. The two coefficient values were used for prediction of productivity decline for these wells. The values of kinetics and formation damage coefficients as obtained from either laboratory or field data vary in the same range intervals. These results validate the proposed mathematical model for sulphate scaling damage and the analytical model-based method "from lab and wells to wells".

1. Introduction

The $Ba/SrSO_4$ scaling is a chronicle disaster in waterflood projects with incompatible injected and formation waters. This phenomenon is attributed to precipitation of barium/strontium sulphate from the mixture of both waters and the consequent permeability reduction resulting in loss of well productivity (Oddo and Tomson, 1994; Sorbie and Mackay, 2000).

The sulphate scaling productivity decline phenomenon has been long recognized in North Sea reservoirs (Mackay et al., 2002) and in Campos Basin fields of Brazil (Bezerra et al., 1996; Rosario and Bezerra, 2001; Gomes et al., 2002).

Decision-making on scale prevention, removal and on stimulation of scaled-up wells is based on scale damage prediction provided by reliable mathematical modelling with coefficients determined from laboratory or field data.

Several numerical (Rocha et al., 2001; Delshad and Pope, 2003; Mackay, 2002) and analytical (Woods and Parker, 2003, Araque-Martinez and Lake, 1999) models describing sulphate scaling under laboratory and field conditions are available in the literature. Chemical reaction options in commercial simulators allow for sulphate modelling on field scale (Eclipse, 2001; Stars, 2003).

Mathematical models for sulphate scaling contain the reaction rate coefficient characterising the intensity of chemical reaction (so called reaction velocity). The reaction rate coefficient is proportional to flow velocity for small velocities, and the proportionality coefficient is called the kinetics coefficient (Fogler, 1998; Lopes, 2002; Bedrikovetsky et al., 2006a,b). The kinetics coefficient is determined by properties of rocks and fluids, by shape of deposit and by thermodynamics conditions.

Another governing parameter is the formation damage coefficient reflecting permeability decrease due to salt precipitation (Pang and Sharma, 1994). The formation damage coefficient also depends on rock and fluid properties. Like permeability or capillary pressure, the kinetics and formation damage coefficients cannot be predicted theoretically for real rocks and fluids.

Scale deposition profile during coreflood is non-uniform because the reagent concentrations decrease along the core due to chemical reaction. So, the sulphate scaling coefficients cannot be directly measured in reactive coreflood tests.

The same applies to scale deposition around production wells.

Therefore, the coefficients must be determined from either laboratory or field data by solution of inverse problems.

* Corresponding author. Tel.: +61(8)83033082.
E-mail addresses: pavel@asp.adelaide.edu.au (P. Bedrikovetsky), monteiro@lenep.uenf.br (R.M.P. Silva), daher@petrobras.com.br (J.S. Daher), zeadilson@petrobras.com.br (J.A.T. Gomes), vcfa@petrobras.com.br (V.C. Amorim).

0920-4105/$ – see front matter © 2009 Elsevier B.V. All rights reserved.
doi:10.1016/j.petrol.2009.06.006

The design and results of barium sulphate quasi-steady state scaling coreflood tests on commingled injection of produced water and seawater have been presented by Read and Ringen (1982), Allaga et al. (1992), Todd and Yuan (1992), Watt et al. (1992), Goulding (1987), Lopes (2002). Breakthrough barium concentration and pressure drop have been measured during the tests for different rocks and fluids.

The analytical model for linear quasi-steady state reactive flow allows calculation of kinetics coefficient from breakthrough barium concentration; the formation damage coefficient is determined from pressure drop rise versus time during the commingled flow of formation water and seawater (Bedrikovetsky et al., 2006a). The laboratory data by Goulding (1987), Yuan (1989), Todd and Yuan (1992), Watt et al. (1992), Lopes (2002) were treated by inverse problem solvers, and the database for sulphate scale coefficients as calculated from twenty-three laboratory tests is presented by Bedrikovetsky et al. (2006b).

In the current paper the methodology of inverse problems based on analytical model for sulphate scaling damage is applied for treatment of well data. An analytical model is derived for quasi-steady state reactive flow towards the well. The inverse problems for sulphate scale damage characterisation are as follows: the kinetics coefficient is calculated from barium concentration in produced water, and the formation damage coefficient is determined from productivity index decline.

Productivity data of five producers from giant offshore field A (Campos Basin, Brazil) submitted to seawater flooding have been treated. The kinetics and formation damage coefficients have been determined and used for prediction of productivity decline in the wells. The scaling damage coefficients have the same orders of magnitude as those obtained from laboratory tests. It allows concluding that it is a sulphate scaling that causes the productivity decline in wells under investigation. It validates the mathematical model for sulphate scaling and justifies using the obtained in laboratory values of sulphate scaling damage coefficients for prediction of well behaviour ("from lab to wells"). It also allows performing the reliable prediction of productivity decline from well production history ("from well to well").

The structure of the work is as follows. In the second section we present mathematical model for sulphate scaling discussing main physics assumptions. An asymptotic analytical model for sulphate scaling near production well, as derived in Appendix B, is presented in Section 3. Two inverse problems for determining the sulphate scale damage coefficients from well productivity history are discussed in fourth section. Fifth section contains results of data treatment from 5 production wells. The comparison between the coefficients as obtained from laboratory and field data is performed in Section 6. The detailed derivations of analytical model are presented in Appendices A to D.

2. Physical schema and mathematical model for sulphate scaling in production wells

We discuss formation damage due to barium sulphate precipitation (oilfield scaling) causing the permeability impairment (Oddo and Tomson, 1994). Usually seawater is injected or co-injected in offshore operations, and it contains SO_4^{2-} anions. If the formation water contains Ba^{2+} cations, mixing of injected and formation waters may cause the $BaSO_4$ deposition (Fig. 1)

$$Ba^{2+} + SO_4^{2-} \rightarrow BaSO_4\downarrow \tag{1}$$

Similar chemical reaction occurs between sulphate cations and strontium, magnesium, calcium and some other anions.

Schema of injected and formation water mixing in a reservoir submitted to waterflooding is shown in Fig. 1. The mixing zone of two waters gradually moves from injector towards producer via different streamlines. Chemical reaction Eq. (1) and consequent precipitation occurs in mixing zone only. Therefore, accumulation of sulphate scale in the reservoir *in situ* does not happen (Sorbie and Mackay, 2000).

Different size streamlines end up in production wells. Simultaneous arrival of displaced formation water via "long" streamlines and of injected seawater via "short" streamlines takes place. It is assumed that wellbore neighbourhood is extremely heterogeneous due to drilling-induced fractures and formation damage. So, under high flow velocity and dispersion near to well, full mixing of waters arriving at producer via different streamlines occurs. Therefore, an intensive water mixing and scale precipitation occurs near to producers.

Fig. 2 shows the schema of commingled oil and water flow towards production well and precipitation of barium/strontium sulphate near to wellbore (Sorbie and Mackay, 2000). The complete mixing of waters is assumed in the mathematical model (Appendix A) that is one-dimensional and operates with concentrations averaged over depth in the well neighbourhood.

The system of governing equations for axisymmetric flow of aqueous solution of barium and sulphate ions with precipitation of solid barium sulphate consists of mass balance equations for barium cation, for sulphate anion, for barium sulphate salt and of Darcy's law accounting for permeability decrease due to scale precipitation (see Philips, 1991; Bedrikovetsky, 1994; Woods and Parker, 2003):

$$\begin{cases} 2\pi r\phi s\dfrac{\partial c_{Ba}}{\partial t} + \dfrac{\partial}{\partial r}\left(Q f c_{Ba} - 2\pi r D\dfrac{\partial c_{Ba}}{\partial r}\right) = -2\pi r K_a c_{Ba} c_{SO_4} \\ 2\pi r\phi s\dfrac{\partial c_{SO_4}}{\partial t} + \dfrac{\partial}{\partial r}\left(Q f c_{SO_4} - 2\pi r D\dfrac{\partial c_{SO_4}}{\partial r}\right) = -2\pi r K_a c_{Ba} c_{SO_4} \\ \phi s\dfrac{\rho_{BaSO_4}}{M_{BaSO_4}}\dfrac{\partial \sigma}{\partial t} = K_a c_{Ba} c_{SO_4} \\ Q = -\dfrac{2\pi r h k_0}{(1+\beta\sigma)}\left(\dfrac{k_{rw}}{\mu_w} + \dfrac{k_{ro}}{\mu_o}\right)\dfrac{\partial p}{\partial r} \end{cases} \tag{2}$$

Here c_{Ba} and c_{SO_4} are barium and sulphate molar concentrations, Q is the flow rate, ϕ is porosity, s is water saturation, K_a is the reaction rate coefficient, σ is the deposited concentration of barium sulphate, ρ_{BaSO_4} and M_{BaSO_4} are barium sulphate density and molecular weight respectively, k_0 is the initial rock permeability, β is the formation damage

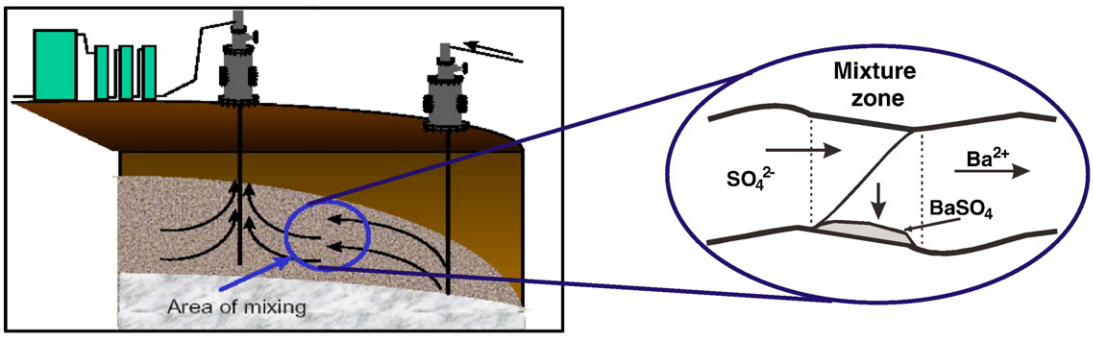

Fig. 1. Precipitation of barium sulphate in the mixing zone inside the stream tube during displacement of formation water by injected seawater.

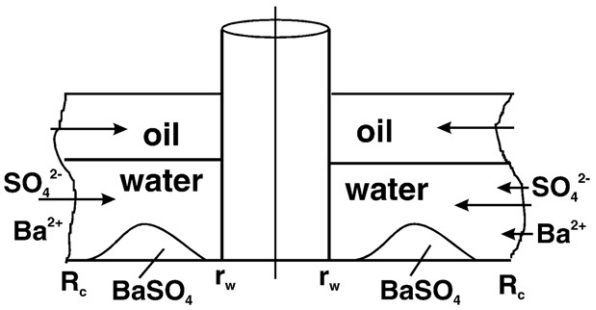

Fig. 2. Schema of simultaneous production of formation and seawaters in well vicinity.

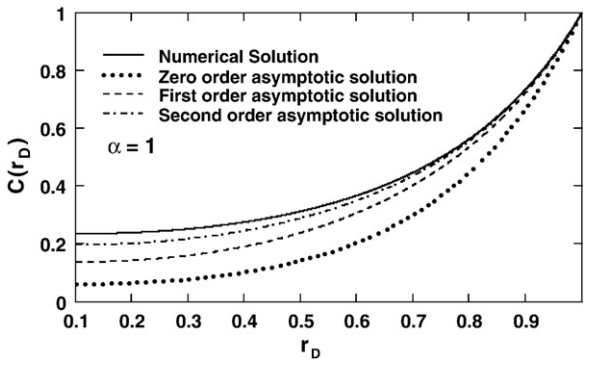

Fig. 3. Barium concentration profile from numerical and asymptotic solutions.

coefficient showing how permeability decreases due to salt deposition, μ is the viscosity, D is the hydrodynamics dispersion.

The chemical reaction rate is given by the law of mass action (Bethke, 1996; Fogler, 1998). The chemical reaction (1) is assumed to be irreversible and have second order.

The model (2) consists of four equations for four unknowns — c_{Ba}, c_{SO_4}, σ and p. The first two equations are independent of σ and p, so they separate from the third and fourth equations.

It is assumed that the dispersion coefficients for Ba^{2+} and SO_4^{2-} ions are equal and proportional to flow velocity, Eq. (A-4); the proportionality coefficient α_D is called dispersivity (Nikolaevskii, 1990). It is also assumed that the chemical reaction constant is proportional to flow velocity for slow non-inertial flows in porous media (Eq. (A-5)), the proportionality coefficient λ is called the kinetics coefficient (Fogler, 1998). The hyperbolic form for permeability decline versus precipitant concentration is assumed, and the formation damage coefficient β characterises how permeability decreases due to precipitation (fourth equation of Eq. (2)).

Between other model assumptions it is worth mentioning the irreversibility of the second order chemical reaction between barium and sulphate ions and independence of the kinetics constant of precipitant concentration (see right hand sides of the first three equations of Eq. (2)).

3. Analytical model for reactive flow around production well

Discuss an analytical model for quasi-steady state reactive flow of incompatible waters towards production well.

A particle moves 1–3 m distance from reservoir up to production well during 8–20 h. The typical period for variation of BSW or of the seawater fraction in produced water is 3–7 months. Therefore, quasi-steady state flow for water and oil in well vicinity is assumed for large time scale, where significant variation of barium or sulphate near to production well occurs.

The speculations are similar to those explaining quasi-steady state pressure distribution around production wells (Dake, 1978).

The fractional flow for water (BSW) is constant for water-oil steady state flows near to producer, see Eqs. (A-1)–(A-3). Therefore, water saturation s is also constant.

The analytical model for quasi-steady state flow around production well is presented in Appendix B. The main model assumptions are based on the facts that salt accumulation during waterflooding occurs mainly near to production wells (Sorbie and Mackay, 2000) and that full mixing of injected and formation waters occurs in the damaged zone.

Steady state distributions of barium and sulphate and barium sulphate accumulation in the production well vicinity is described by the system of two ordinary differential equations (B-1) subject to boundary conditions (A-8) and (A-9).

The steady state model can be applied for short periods between well stimulations, which in the field under consideration usually takes place once in 6–10 months. In this case we assume BSW and both reagent concentrations to be constant.

Considering the longer periods, we use the steady state solution (C-3, C-5, C-7) obtained under assumptions that BSW f and inlet concentrations C and Y are constants, and insert time-dependencies $c^0_{Ba}(t)$ and $c_{SO_4^0}(t)$ into the formulae.

The deposited concentration accumulates proportionally to time, Eq. (C-9). It also corresponds to short time periods. For large time scales, time dependencies $f(t)$, $c^0_{Ba}(t)$ and $c_{SO_4^0}(t)$ are used during integration in time of the third equation (Eq. (A-7)).

Usually sulphate concentration in seawater is around 3000 ppm, barium concentration in formation water rarely exceeds 150 ppm. So, in majority of cases sulphate concentration highly exceeds that of barium, $\alpha \ll 1$, and asymptotic method (C-1) can be applied.

The asymptotic solution is obtained in Appendix C up to second order approximation. Zero, first and second order approximations are expressed by explicit formulae (C-3), (C-5) and (C-7).

Fig. 3 shows barium concentration profile along the path from the reservoir towards the production well. Barium concentration decreases along the path due to chemical reaction with sulphate.

Four curves in Fig. 3 correspond to zero-, first- and second order approximations; the continuous curve was calculated numerically using 4th order Runge–Kutta method. Just to evaluate asymptotic formula (C-1) as a predictive tool, the "worse" case on the limit of convergence $\alpha = 1$ is discussed. Even in this case, the second order approximation gives 15% error in prediction of barium concentration in produced water; first order approximation provides with 40% error and zero order gives 75% error.

Fig. 4 shows the error in barium concentration profile by zero-, first- and second order approximations (C-1), (C-3), (C-5) and (C-7) if compared with numerical solution shown by continuous curve. For a typical case of initial concentration ratio $\alpha = 0.1$, error for second order approximation is less than 0.1%; first order approximation provides with the error 1.3% while zero order approximation gives 14%. So, asymptotic

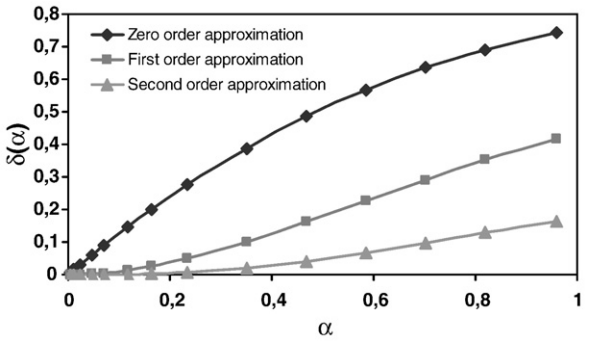

Fig. 4. Function of relative error between numerical and asymptotic solutions versus concentrations ration α.

analytical model (C-1)–(C-7) predicts reagent concentration profiles near to well with good accuracy.

Fig. 5a shows barium concentration profiles around production well. The profiles are steady state, i.e. all newly arriving reagents precipitate. Four curves correspond to different values of kinetics coefficient. Table 1 presents values of kinetics and formation damage coefficients as obtained from four sets of laboratory tests. The chosen four values of kinetics coefficient in Fig. 5a represent the whole variation interval of λ.

The higher is the kinetics number the lower is the barium concentration profile. It is important to emphasise, that even for low kinetics constant value, barium concentration in produced water does not exceed 0.01 of the barium concentration on the contour R_c. From the value $\lambda = 400\,(\mathrm{M\ m})^{-1}$ up, barium concentration almost disappears before water arrival to production well.

Typical values of barium concentration in formation water of Campos Basin fields vary from 30 to 150 ppm. Barium concentration in produced water varies from 2 to 5 ppm. The orders of magnitude for barium concentration in produced water from field data agree with those in Fig. 5a.

Sulphate concentration Y also decreases from contour to well due to chemical reaction. Therefore, the product of ion concentrations in formula for deposited concentration (C-9) decreases as kinetics coefficient λ increases. From another side, the deposition rate is proportional to λ, see Eqs. (2) and (A-5). It results in non-monotonic dependency of deposited concentration versus kinetics coefficient.

Fig. 5b shows the dependency S versus λ in point $r_D = 0.5$ for three moments $t_D = 5000$, 15,000 and 50,000 pvi (here the contour radius was taken as that of the damaged zone, $R_c = 1$ m, (A-7)). The deposited concentration tends to zero for either weak or intensive reactions, where the kinetics number ε_k tends either to zero or to infinity. Maximum deposited concentration is realized for some intermediate kinetics coefficient value.

Calculations of pressure drop between the contour and the well use the pressure gradient expression as obtained from modified

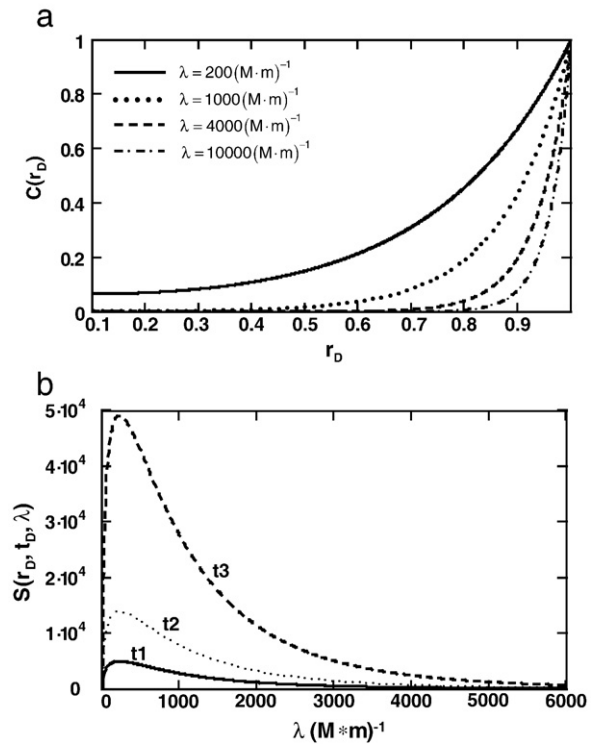

Fig. 5. Barium and barium sulphate concentrations: a) barium concentration profile versus dimensionless radius for different λ in 1 m well neighbourhood, b) dependency of the deposit concentration on kinetics coefficient.

Table 1
Values of kinetics and formation damage coefficients as obtained from corefloods.

Coreflood test	Kinetics coefficient λ $(\mathrm{M\ m})^{-1}$	Formation damage coefficient β
Lopes (2002)	3003–3951	–
Yuan (1989)		
Test at 20 °C	239–18585	10–100
Test at 70 °C	1553–42200	20–100
Goulding (1987)	32,000–184,000	30–3000
Watt et al. (1992)	798–963	–

Darcy's law, fourth equation (Eq. (2)). The dimensionless pressure drop normalised by those at the absence of formation damage (so called impedance) is calculated in Appendix D, see Eq. (D-6):

$$J(t_D) = 1 + mt_D$$

$$m = \beta c^0_{Ba}\frac{M_{BaSO_4}}{\rho_{BaSO_4}}\frac{1}{2\ln\left(\frac{R_c}{r_w}\right)}\frac{f}{s}M(\varepsilon_k,\alpha), M(\varepsilon_k,\alpha) = \varepsilon_k\int_{\frac{r_w}{R_c}}^{1}\frac{C(r_D)\cdot Y(r_D)}{r_D^2}dr_D \quad (3)$$

The impedance grows linearly with time. The proportionality coefficient m is called the impedance slope.

Like steady state distributions of reagent concentrations (C-1), formula (3) is valid for short time periods where BSW and inlet concentrations for barium and sulphate are constant. For large time scales where barium and sulphate concentrations along with BSW are not constant, time dependencies $f(t)$, $c^0_{Ba}(t)$ and $c_{SO_4^{2-}}(t)$ must be used during integration (D-1).

The impedance slope can be expressed via skin factor (Dake, 1978)

$$S_f = \frac{m}{2}\ln\left(\frac{R_c}{r_w}\right)t_D \quad (4)$$

The impedance slope is proportional to formation damage coefficient β, see Eq. (3). Therefore, the β-value highly affects well productivity decline due to sulphate scaling.

Formula (4) shows that skin factor grows proportionally to time.

Fig. 6 shows decrease of productivity index for different kinetics coefficients and for formation damage coefficient $\beta = 300$. The value $\beta = 300$ corresponds to moderate formation damage, $\lambda = 500$ and $\lambda = 10{,}000$ are low and large values respectively (Table 1). The dimensionless time is calculated for drainage radius $R_c = 500$ m. The inlet sulphate concentration is 3000 ppm that is a typical for seawater. So, it is assumed that sulphate loss due to chemical reaction in the reservoir can be ignored. The inlet barium concentration is 80 ppm, which also means that chemical reaction occurs mainly near to well.

As it is shown in Fig. 6, the higher is the kinetics coefficient the faster is the productivity decline. The significant productivity decline occurs already after production of 0.001 pvi

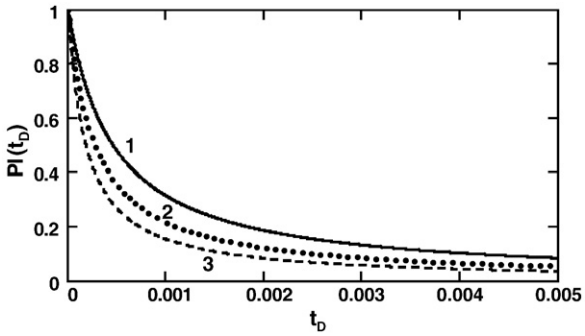

Fig. 6. Dynamics of *PI* decline for different values of chemical kinetics coefficient λ. Here: 1 − $\lambda = 500\,(\mathrm{M\ m})^{-1}$; 2 − $\lambda = 4000\,(\mathrm{M\ m})^{-1}$; 3 − $\lambda = 10000\,(\mathrm{M\ m})^{-1}$.

4. Characterisation of sulphate scaling damage from well/field data

Consider sulphate scaling damage characterisation from histories of well productivity decline and of barium concentration in produced water, based on the analytical model for reactive flow towards well. The characterisation includes calculation of kinetics coefficient λ and formation damage coefficient β.

Barium concentration in produced water $C(r_w/R_c)$ can be calculated from analytical solution (C-3), (C-5) and (C-7). The concentration $C(r_w/R_c)$ is equal to that at the contour R_c [$C=1$] for the case of weak chemical reaction, $\lambda=0$. The higher is the kinetics coefficient λ the lower is barium concentration in produced water. Therefore, kinetics coefficient can be determined from barium concentration in produced water $C(r_w/R_c)$.

The solution exists under natural assumptions; it is unique and stable with respect to small perturbations (Alvarez et al., 2006a).

The method for calculation of kinetics coefficient using barium concentration in produced water is based on analytical solution of reactive flow equation around production wells. Either of approximations (C-3), (C-5) and (C-7) is a transcendental equation with respect to kinetics number ε_k. The kinetics coefficient λ is calculated via ε_k using dimensionless expression (A-6).

The higher is the formation damage coefficient the higher is impedance slope m. If precipitation does not damage the rock, $\beta=0$, impedance is constant and $m=0$. Therefore, the formation damage coefficient can be determined from impedance slope m, Eq. (3).

The solution also exists, is unique and stable (Alvarez et al., 2006b).

The analytical axisymmetric model and corresponding inverse problems are similar to those for corefloods (Bedrikovetsky et al., 2006a,b).

The model (2) is one-dimensional, i.e. vertical diffusive flux between layers with different permeability instantly makes the depth concentration distribution uniform. Also, it is assumed that reaction is

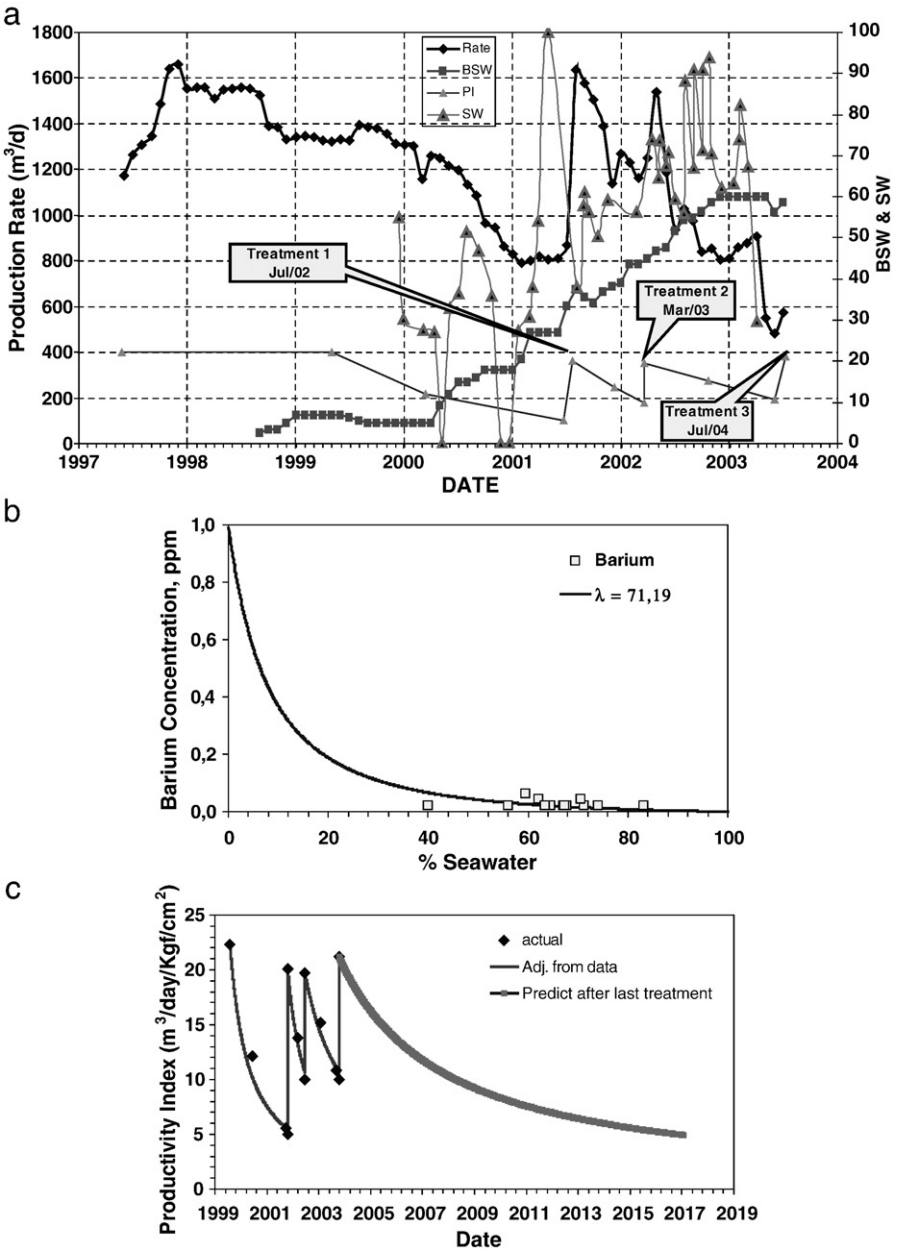

Fig. 7. Treatment of production well data from field A: a) history of BSW, production rate, seawater fraction in produced water and productivity index, b) concentration of barium ions in produced water versus seawater fraction; c) treatment of three periods of *PI* decrease and prediction for the fourth period.

occurring only near to production wells. This assumption limits the model applicability. Nevertheless, while not being able to determine the exact values for scaling damage parameters from well data, the model does provide us with their order of magnitude.

In the next section we consider the case where scaling happens mainly in gravel pack and in the close well neighbourhood (Gomes et al., 2002; Daher et al., 2005) and 1d model (2) is valid.

5. Determination of kinetics and formation damage coefficients from field data

In this section we calculate two sulphate scale damage coefficients for five wells using the solutions of two inverse problems presented in the previous section.

Figs. 7 and 8 present data for highly permeable, low heterogeneity, large net pay offshore sandstone field A (Campos Basin, Brazil). Production well A1 is completed by gravel pack where intensive barium sulphate accumulation takes place due to high flow velocity and, consequently, high dispersion and reaction rate coefficient. It confirms the model assumption that significant chemical reaction and deposition occurs only in the well vicinity (Gomes et al., 2002 and Daher et al., 2005). Reservoir modelling with barium sulphate reaction for field A shows that bulk of chemical reaction occurs in 1 m neighbourhood of producers; the injected solvent removed sulphate scale in 1 m radius from the well. The papers also neglect decrease of reagent concentrations due to chemical reaction in the reservoir if compared with those occurring near to wellbore and in the gravel pack. Works by Gomes et al. (2002) and Daher et al. (2005) state that for the case of two producers from field A, where the major precipitant accumulation occurs near to well and in the gravel pack, the 1d model (2) is valid for this case. It justifies application of the analytical axisymmetric reactive flow model (C-1)–(C-9), (3) in the analysis of well histories.

One can also notice the large scattering of seawater fraction in the produced water (Fig. 7). Variation of averaged monotone seawater fraction during intervals between well treatments is significantly lower than that of raw data. It also justifies using the analytical model with constant BSW and inlet reagent concentrations during short periods between stimulations.

In all well data treatments, the mean values for water cut, saturation and inlet concentrations, for time periods between well stimulations, were used.

Fig. 7a presents histories of BSW, seawater fraction in produced water, production rate and productivity index for well A1. The history of productivity index (PI) is also shown in Fig. 7c. The water breakthrough happened in August 1998 (see BSW-curve); the rate and productivity index decline started in May 1999 (see PI-curve in Fig. 7a and c). The explanation of the delay is as follows. During short period after the breakthrough, just formation water is produced; the seawater appears in produced fluid after the production of formation water bank (Sorbie and Mackay, 2000). Therefore, scale formation with consequent productivity index losses starts with some delay if compared with the breakthrough time.

Three different time intervals with gradual productivity index decline and its instant rise correspond to history of scale formation between three well treatments (Fig. 7a and c).

Fig. 7b shows decrease of barium in produced water during increase of seawater fraction in produced water. Barium concentration at the outer damaged zone boundary R_c is assumed to be equal to its initial concentration because all sulphate scale is formed in the well neighbourhood and in the gravel pack. Each "produced" barium point allows calculation of kinetics constant. We use all points and achieve the best fit by the curve that corresponds to the constant λ in each of three time intervals.

Indeed, the same λ-value of kinetics coefficient adjusts the overall curve in three time intervals.

The thermodynamic conditions (temperature and ionic strength) are the same in time intervals before and after the treatments. Assume that the treatments do not alternate deposition conditions on matrix surface. It explains why the kinetics constant is the same for all time intervals.

The best fit of the curve "barium concentration in produced water versus seawater fraction in produced water" by formulae (C-1) and (C-7) using least square method was achieved for $\lambda = 71.19\ (\mathrm{M\ m})^{-1}$.

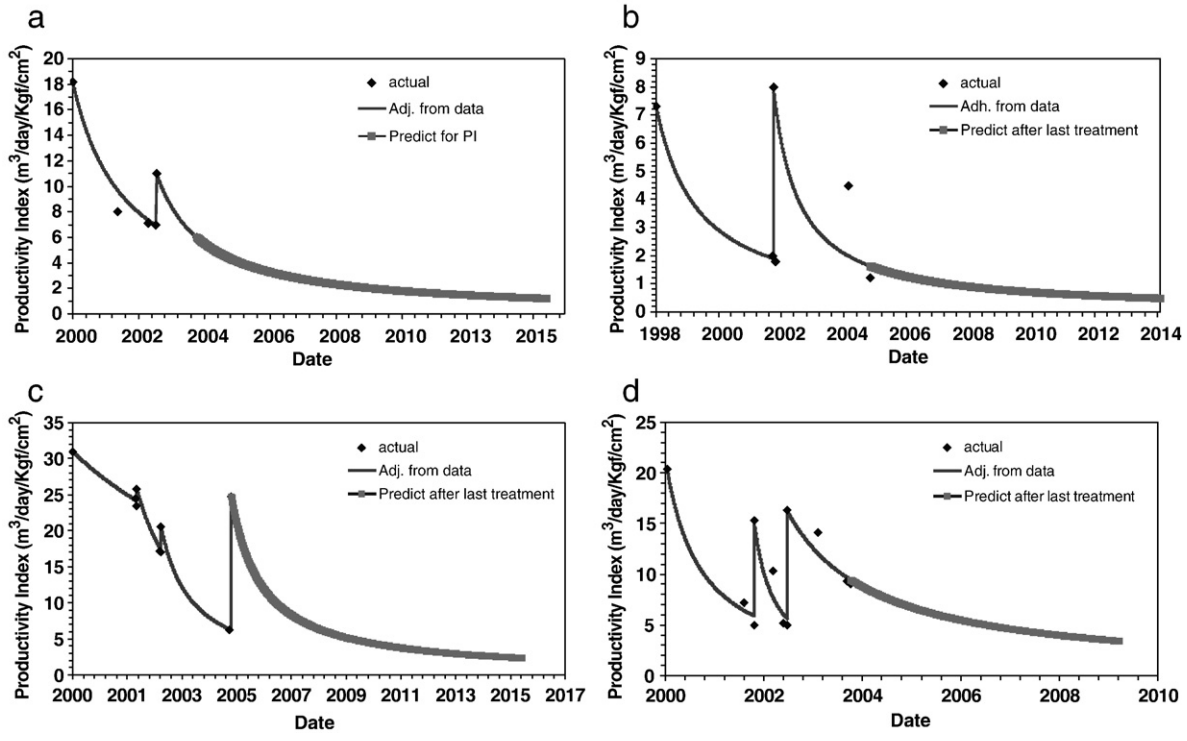

Fig. 8. Treatment of four well data from field A and prediction of productivity index.

Table 2
Values of kinetics and formation damage coefficients as obtained from field data.

	Kinetics coefficient λ	Formation damage coefficient		
	$(M\ m)^{-1}$	β_1	β_2	β_3
Well 1	312.78	8.67	5.41	–
Well 2	147.22	38.22	46.28	–
Well 3	72.61	5.73	16.32	40.97
Well 4	71.19	166	39.04	18.32
Well 5	166.98	49.88	77.66	5.68

The formation damage coefficient was obtained by adjustment of the productivity index curve using formula (3). Three interval fittings (Fig. 7c) result in three values for formation damage coefficient: $\beta = 166$, 39 and 18.

Table 1 shows that the variation interval of formation damage coefficient as obtained from laboratory tests is [30,3000] (Bedrikovetsky et al., 2006b).

We attribute the obtained small values of the formation damage coefficient to the fact that precipitation occurs mostly near to wellbore and in the gravel pack for the well discussed. The porous media in the field A and in the gravel pack are highly permeable, so some permeability decline occurs only after significant deposition.

The known values of kinetics and formation damage coefficients allow predicting the producer behaviour using the analytical model. After the third treatment, PI increases from 10.8 to 21.2 $(m^3/day)/(kgf/cm^2)$. The fourth interval of productivity index decline corresponds to predictive modelling (Fig. 7c). It was noticed that formation damage coefficient decreases from treatment to treatment; so, we fixed $\beta = 13$ for predictive period. After 53 months during the predictive period, the productivity index decreases twice (Fig. 7c).

Fig. 8a,b,c,d presents results of treatment of productivity data and productivity decline prediction for other four wells from the field A.

The data for kinetics constant and formation damage coefficient as obtained from five wells are presented in Table 2. The fact that formation damage coefficient as obtained from different time periods between well treatments for the same well varies significantly while the kinetics coefficient is almost constant was observed for four other wells also.

Daher et al., 2006, presented experience of scale removal by solvent in scaled-up wells of the field A. Prediction of productivity decline in five wells (Figs. 7c and 8) allows planning of further well treatments like scale removal and acidification.

6. Comparison between laboratory and field data

Let us compare the values of kinetics and formation damage coefficients as obtained from laboratory and field data.

Multiple completely different physics-chemical mechanisms can cause productivity damage — pore collapse, rock deformation, fines migration, asphaltene deposition, etc. (Civan, 2000). The correct diagnosis of formation damage in specific field results in right decision-making on damage prevention or removal.

Determination of model coefficients from inverse problems using laboratory and field data and their comparison is an important method for the damage diagnosis. Difficulties in well intervention for deep-water fields like field A make this method to be the most important.

Comparison between the kinetics and formation damage coefficients as obtained from laboratory and field data may resolve the doubt whether it is a sulphate scaling that causes productivity decline in the fields under investigation.

Values of kinetics constant λ and formation damage coefficient β as obtained from laboratory data are presented in Table 1. Histograms for two coefficients are given in Fig. 9.

The kinetics coefficient depends on temperature and on ionic strength of brines. Therefore, it varies from test to test performed under different thermodynamic conditions. Unfortunately, the laboratory data sufficient for correlation between the kinetics coefficient and the temperature and ionic strength of brines are unavailable in the literature. Therefore, the obtained values are summarized in a single Table 1 and in Fig. 9 without specifying the thermodynamics conditions. It explains the wide interval of kinetics constant variation.

Large interval for λ variation is also caused by unknown dispersion coefficient in majority of tests; the results include λ-values as calculated for three dispersion coefficients $\alpha_D = 0.005$, 0.01 and 0.03 m. The dispersion coefficient with scaling coreflood was measured only by Lopes, 2002. The dispersivity coefficient for two cores was $\alpha_D = 0.011$ and 0.018 m. So the values $\lambda = 3003$ and $\lambda = 3951$ obtained in this work for two cores are more reliable.

The results of well data treatment for barium concentration in produced water are presented in Table 2. The thermodynamic conditions for temperature and brine ionic strength are the same for the wells of the same reservoir, so the obtained λ-values present less scattering than those presented in Fig. 9 — the variation interval for kinetics coefficient is [71,313]. This variation interval fits to that presented in Table 1 and in Fig. 9 for laboratory data.

The values of formation damage coefficient as obtained from productivity index decline for five wells are presented in Table 2. The data from periods between well treatments were processed separately. For wells A1 and A2 data for two time periods are available (Fig. 8a and b), for wells A3, A4 and A5 three period data are presented in Figs. 8c, 7c and 8d respectively. So, 13 values of formation damage coefficients are presented in Table 2.

Formation damage coefficient depends on the type of solid deposit on grain surface. Permeability reduction due to dendrite growth or pore bridging is orders of magnitude higher than those due to pore lining or filling (Dunn et al., 1991; Nancollas and Liu, 1975; Oren and Bakke, 2002). It explains large variation of β-values obtained from laboratory data (Table 1).

Despite the above-mentioned uncertainties, the values of formation damage coefficients as obtained from well data vary in smaller

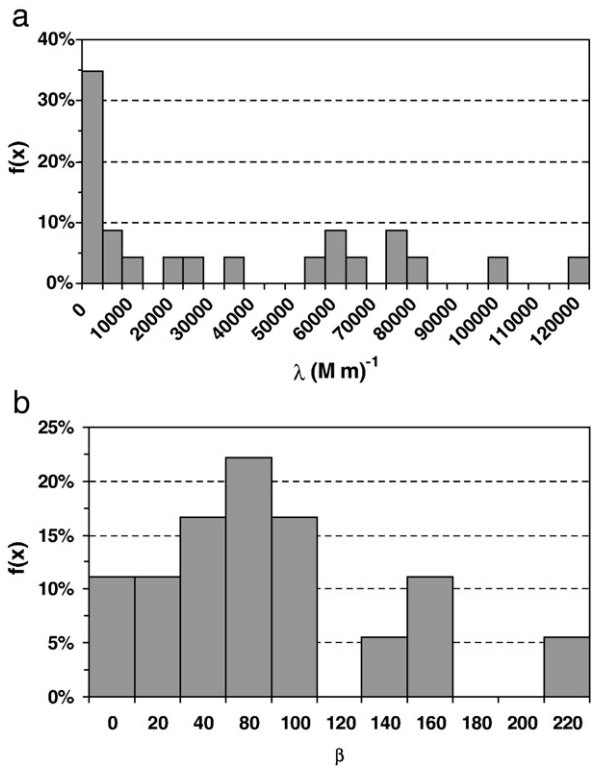

Fig. 9. Distribution functions for kinetics coefficient λ $(M\ m)^{-1}$ and for formation damage coefficient β as obtained from laboratory tests.

interval [6,166] than that for corefloods [30,3000]. It can be attributed to similar rock morphology for wells from the same field.

The intervals for formation damage coefficients as obtained from sulphate scaling laboratory and field data coincide with those obtained for injectivity decline processes (Pang and Sharma, 1994).

As it was mentioned before, the variation intervals for sulphate scaling damage coefficients are wide due to uncertainty in thermodynamic conditions and rock morphology for laboratory tests and production wells. Nevertheless, comparison between the coefficients as calculated from two sources shows that they have the same order of magnitude. Under the present high level of result scattering, it allows concluding that the sulphate scaling is the cause for productivity decline in wells under investigation. Besides, the reactive transport model in porous media (2) is an adequate model for prediction of productivity decline in scaled-up wells. It validates using two model coefficients as obtained from laboratory data for prediction of productivity decline in scaled-up producers "from lab to wells". It also justifies the method of determining the sulphate scaling damage coefficients from well productivity data and using the coefficient values for forecasting further well productivity decline ("from well to well").

The λ and β values obtained from laboratory data (Table 1) and from well histories (Table 2) can be recommended for feasibility studies and sensitivity analysis by reservoir simulation when coreflood or well production data are unavailable.

7. Summary

Five scaled-up producers with declined productivity are analysed in order to predict productivity index and to plan the well stimulation program. The wells are completed by gravel packs. Complete mixing of sea- and formation waters in production well neighbourhoods in the reservoir under consideration was assumed in previous works. Using this assumption, quasi-steady state model for reactive flow around production well is formulated. Asymptotic solution allows derivation of explicit formulae for concentrations and productivity index.

The analytical model shows that reciprocal of productivity index is proportional to production time, and the proportionality coefficient is mostly affected by formation damage coefficient.

The sulphate scaling damage parameters are determined from production data: the kinetics coefficient is found from barium concentration in produced water, and the formation damage coefficient is determined from productivity index decline.

The formation damage coefficients as obtained from different periods between stimulations of the same well are different, allowing to conclude that every stimulation changed the pore space. Nevertheless, the kinetics coefficients as obtained from different periods of the same well are almost equal that permit concluding that kinetics of the barium-sulphate reaction is independent of the rock structure.

Both coefficient values as determined for five wells are inside the variation intervals for scale damage coefficients obtained from coreflood data.

It allows concluding that the productivity damage in wells under investigation was caused by sulphate scaling and validates the mathematical model. It also permits to perform a reliable prediction of well productivity. The values for kinetics and formation damage coefficients as obtained from well and laboratory data are recommended for use in reservoir modelling of sulphate scaling.

Acknowledgements

The authors thank Dr. Francisca Rosario (Petrobras) and Prof. Eric Mackay (Heriot Watt U., UK) for fruitful discussions. Many thanks are due to Prof. Themis Carageorgos (University of Adelaide, Australia) for support and encouragement.

Appendix 1. Appendix A Derivation of governing equations

Production rates of oil and water are

$$Q_w = fQ,\ Q_o = (1-f)Q \tag{A-1}$$

where f is a fractional flow for water that depends on water saturation and on the precipitant concentration:

$$f = \frac{\frac{k_{rw}(s,\sigma)}{\mu_w}}{\frac{k_{rw}(s,\sigma)}{\mu_w} + \frac{k_{ro}(s)}{\mu_o}} = f(s,\sigma) \tag{A-2}$$

From Eq. (A-1) follows that fractional flow is constant for steady state flow of water and oil:

$$f(s,\sigma) = Q_w/Q = f \tag{A-3}$$

The axisymmetric system (2) describes one-dimensional reactive flow during waterflooding in production well vicinity. Here the law of mass action is assumed for the chemical reaction (salt deposition) rate (Fogler, 1998; Bethke, 1996).

The system of four equations (Eq. (2)) is closed. The unknowns are three concentrations c_{Ba}, c_{SO_4}, σ, and pressure p.

It is assumed that the diffusion coefficients for Ba^{2+} and SO_4^{2-} ions in aqueous phase are equal and proportional to flow velocity (Nikolaevskii, 1990):

$$D_{Ba} \cong D_{SO_4} \cong D \cong \alpha_D f U \tag{A-4}$$

The proportionality between the chemical reaction rate constant K_a and water flow velocity was observed for reactive flows in general (Fogler, 1998) and particularly for sulphate scaling reactions (Lopes, 2002; Bedrikovetsky et al., 2006a):

$$K_a = \lambda f U \tag{A-5}$$

Let us introduce the following dimensionless co-ordinates and parameters:

$$t_D = \frac{Qt}{\pi R_c^2 h\phi},\ r_D = \frac{r}{R_c},\ C = \frac{c_{Ba}}{c_{Ba}^0},\ Y = \frac{c_{SO_4}}{c_{SO_4}^0},\ S = \frac{\rho_{BaSO_4}}{M_{BaSO_4}}\frac{\sigma}{c_{Ba}^0}$$
$$p_D = \frac{2\pi h k_o}{Q}\left(\frac{k_{rw}}{\mu_w} + \frac{k_{ro}}{\mu_o}\right)p,\ \alpha = \frac{c_{Ba}^0}{c_{SO_4}^0},\ \varepsilon_D = \frac{\alpha_D}{R_c},\ \varepsilon_k = \lambda R_c c_{SO_4}^0 \tag{A-6}$$

Substituting dimensionless co-ordinates and parameters (A-6) in the system of governing equations (Eq. (2)), we obtain:

$$\begin{cases} 2r_D\frac{s}{f}\frac{\partial C}{\partial t_D} + \frac{\partial}{\partial r_D}\left(C - \varepsilon_D\frac{\partial C}{\partial r_D}\right) = -\varepsilon_k CY \\ 2r_D\frac{s}{f}\frac{\partial Y}{\partial t_D} + \frac{\partial}{\partial r_D}\left(Y - \varepsilon_D\frac{\partial Y}{\partial r_D}\right) = -\varepsilon_k \alpha CY \\ 2r_D\frac{s}{f}\frac{\partial S}{\partial t_D} = \varepsilon_k CY \\ 1 = -\frac{r_D}{\left(1 + \beta c_{Ba}^0\frac{M_{BaSO_4}}{\rho_{BaSO_4}}S\right)}\frac{dp_D}{dr_D} \end{cases} \tag{A-7}$$

The boundary condition on the well corresponds to the absence of diffusive flux for either specie:

$$r_D = \frac{r_w}{R_c} : \frac{dC}{dr_D} = \frac{dY}{dr_D} = 0 \qquad (A-8)$$

The contour boundary condition corresponds to given barium and sulphate concentrations:

$$r_D = 1 : C - \varepsilon_D \frac{\partial C}{\partial r_D} = 1,\ Y - \varepsilon_D \frac{\partial Y}{\partial r_D} = 1 \qquad (A-9)$$

Appendix 2. Appendix B Solution for steady state flow with chemical reaction

It was assumed that the effect of precipitated barium sulphate on the fractional flow function is negligible. In this case, saturation is constant. First two equations (A-7) are separated from accumulation equation and modified Darcy's law. Let us consider steady state flow in well vicinity:

$$\begin{cases} \dfrac{dC}{dr_D} = \varepsilon_D \dfrac{d^2C}{dr_D^2} - \varepsilon_k CY \\ \dfrac{dY}{dr_D} = \varepsilon_D \dfrac{d^2Y}{dr_D^2} - \varepsilon_k \alpha CY \end{cases} \qquad (B-1)$$

Boundary conditions (A-8) and (A-9) correspond to steady state distribution of both reagents during reactive flow near to production well.

Introduce the following linear combination of two concentrations:

$$V(r_D) = C(r_D) - \frac{Y(r_D)}{\alpha} \qquad (B-2)$$

The equation for $V(r_D)$ is obtained by subtraction the second equation (B-1) from the first equation (B-1):

$$\frac{dV}{dr_D} = \varepsilon_D \frac{d^2V}{dr_D^2} \qquad (B-3)$$

Boundary conditions for $V(r_D)$ follows from Eqs. (A-8) and (A-9):

$$r_D = \frac{r_w}{R_c} : \frac{dV}{dr_D} = 0 \qquad (B-4)$$

$$r_D = 1 : V = 1 - \frac{1}{\alpha} \qquad (B-5)$$

The solution for boundary problem (B-3) to (B-5) is constant:

$$V(r_D) = 1 - \frac{1}{\alpha} \qquad (B-6)$$

Expressing Y via C from Eq. (B-2) and substituting it into the first equation (Eq. (B-1)), we obtain a second order ordinary differential equation for unknown $C(r_D)$:

$$\varepsilon_D \frac{d^2C}{dr_D^2} - \frac{dC}{dr_D} - \varepsilon_k C[1 + \alpha(C-1)] = 0 \qquad (B-7)$$

Eq. (B-7) is subject to boundary conditions (A-8, A-9) for unknown function $C = C(r_D)$.

Appendix 3. Appendix C Asymptotic solution for concentration profiles

Usually the sulphate concentration in seawater significantly exceeds the barium concentration in formation water. In this case, parameter α is negligibly small, $\alpha \ll 1$, Eq. (A-6). Let us find asymptotic solution for the steady state flow problem (A-8), (A-9), and (B-7) for small parameter α:

$$C(r_D) = C_0(r_D) + \alpha C_1(r_D) + \frac{\alpha^2}{2} C_2(r_D) \qquad (C-1)$$

The term $[C(x_D) - 1]$ varies from minus unity to zero, so the second term in brackets on the right hand side of Eq. (B-7) can be neglected comparing with unity. Substituting expansion (C-1) into Eq. (B-7) obtain a linear second order ordinary differential equation for zero order approximation:

$$\varepsilon_D \frac{d^2C_0}{dr_D^2} - \frac{dC_0}{dr_D} - \varepsilon_k C_0 = 0 \qquad (C-2)$$

The boundary problem (A-8) and (A-9) for Eq. (C-2) allows for exact solution:

$$C_0(r_D) = \frac{\Gamma_1 \exp[\Gamma_2 r_D] - \Gamma_2 \exp\left[(\Gamma_2 - \Gamma_1)\dfrac{r_w}{R_c} + \Gamma_1 r_D\right]}{\Gamma_1 \exp[\Gamma_2] - \Gamma_2 \exp\left[(\Gamma_2 - \Gamma_1)\dfrac{r_w}{R_c} + \Gamma_1\right]} \qquad (C-3)$$

$$\Gamma_1 = \frac{1}{2\varepsilon_D} + \sqrt{\frac{1 + 4\varepsilon_D\varepsilon_k}{4\varepsilon_D^2}}$$

$$\Gamma_2 = \frac{1}{2\varepsilon_D} + \sqrt{\frac{1 + 4\varepsilon_D\varepsilon_k}{4\varepsilon_D^2}}$$

The equation for first order approximation is:

$$\varepsilon_D \frac{d^2C_1}{dr_D^2} - \frac{dC_1}{dr_D} - \varepsilon_k C_1 - \varepsilon_k C_0^2 + \varepsilon_k C_0 = 0 \qquad (C-4)$$

Substituting expansion (C-1) into boundary conditions (A-8), (A-9) and integration of linear non-homogeneous equation (C-4), obtain first order approximation:

$$C_1(r_D) = c_1 e^{\Gamma_1 r_D} + c_2 e^{\Gamma_2 r_D} + K_1 e^{2\Gamma_1 r_D} + K_2 e^{(\Gamma_1 + \Gamma_2) r_D} + K_3 e^{2\Gamma_2 r_D} + K_4 r_D e^{\Gamma_1 r_D} + K_5 r_D e^{\Gamma_2 r_D} \qquad (C-5)$$

Here constants c_1 and c_2 are obtained from boundary conditions; constants $K_1, K_2 \ldots K_5$ are calculated during solution of inhomogeneous linear equation (C-4) where C_0 is a zero order approximation (C-3).

The equation for second order approximation is also obtained by substitution of expansion (C-1) into Eq. (B-7):

$$\varepsilon_D \frac{d^2C_2}{dr_D^2} - \frac{dC_2}{dr_D} - \varepsilon_k C_2 + 2\varepsilon_k C_1 - 4\varepsilon_k C_0 C_1 = 0 \qquad (C-6)$$

The solution provides with second order approximation

$$\begin{aligned} C_2(r_D) = {} & c_3 e^{\Gamma_1 r_D} + c_4 e^{\Gamma_2 r_D} + (m_0 + m_1 r_D) e^{2\Gamma_1 r_D} \\ & + (m_2 + m_3 r_D) e^{(\Gamma_1 + \Gamma_2) r_D} \\ & + (m_4 + m_5 r_D) e^{2\Gamma_2 r_D} + (m_6 + m_7 r_D) r_D e^{\Gamma_1 r_D} \\ & + (m_8 + m_9 r_D) r_D e^{\Gamma_2 r_D} + n_1 e^{(2\Gamma_1 + \Gamma_2) r_D} \\ & + n_2 e^{(\Gamma_1 + 2\Gamma_2) r_D} + n_3 e^{3\Gamma_1 r_D} + n_4 e^{3\Gamma_2 r_D} \end{aligned} \qquad (C-7)$$

Expression for sulphate concentration profile is obtained from barium profile using Eqs. (B-2) and (B-6)

$$Y(r_D) = \alpha(C(r_D) - 1) + 1 \qquad (C-8)$$

Integrating third equation (A-7) in t_D, obtain deposited concentration $S(r_D,t_D)$:

$$S(r_D,t_D) = \frac{\varepsilon_k}{2r_D}\frac{f}{s}C(r_D)Y(r_D)t_D \qquad (C-9)$$

Appendix 4. Appendix D Productivity index calculations

Let us calculate the pressure drop between the contour and the well using the pressure gradient expression as obtained from modified Darcy's law, fourth equation of Eq. (2).

$$\Delta p = \int_{r_w}^{R_c} -\frac{dp}{dr}dr = \frac{Q}{2\pi hk_0}\left(\frac{k_{rw}}{\mu_w}+\frac{k_{ro}}{\mu_o}\right)^{-1}\int_{r_w}^{R_c}\frac{1+\beta\sigma}{r}dr$$

$$= \frac{Q}{2\pi hk_0}\left(\frac{k_{rw}}{\mu_w}+\frac{k_{ro}}{\mu_o}\right)^{-1}\left(\ln\left(\frac{R_c}{r_w}\right)+\beta c^0_{Ba}\frac{M_{BaSO_4}}{\rho_{BaSO_4}}\int_{\frac{r_w}{R_c}}^{1}\frac{S(r_D,t_D)}{r_D}\right)dr_D \qquad (D-1)$$

Substituting dimensionless deposited concentration, as obtained from third equation (A-7), into the second integral in brackets (D-1), we obtain expression for the integral:

$$\int_{\frac{r_w}{R_c}}^{1}\frac{S(r_D,t_D)}{r_D}dr_D = \frac{\lambda R_c c^0_{SO_4}}{2}\frac{f}{s}t_D\int_{\frac{r_w}{R_c}}^{1}\frac{C(r_D)\cdot Y(r_D)}{r_D^2}dr_D \qquad (D-2)$$

The final expression for the pressure drop is:

$$\Delta p = \frac{Q}{2\pi hk_0}\left(\frac{k_{rw}}{\mu_w}+\frac{k_{ro}}{\mu_o}\right)^{-1}\left(\ln\left(\frac{R_c}{r_w}\right)+\beta c^0_{Ba}\frac{M_{BaSO_4}}{\rho_{BaSO_4}}\frac{\varepsilon_k}{2}\frac{f}{s}t_D\int_{\frac{r_w}{R_c}}^{1}\frac{C(r_D)\cdot Y(r_D)}{r_D^2}dr_D\right) \qquad (D-3)$$

At $t_D=0$ expression (D-3) degenerates to the Dupui formula for productivity index:

$$Q = \frac{2\pi hk_0}{\ln\left(\frac{R_c}{r_w}\right)}\left(\frac{k_{rw}}{\mu_w}+\frac{k_{ro}}{\mu_o}\right)\Delta p \qquad (D-4)$$

Formula for productivity index is

$$PI = \frac{Q}{\Delta P} \qquad (D-5)$$

Finally, dimensionless inverse to productivity index (impedance) is:

$$\frac{PI^0}{PI} = 1+\left(\beta c^0_{Ba}\frac{M_{BaSO_4}}{\rho_{BaSO_4}}\frac{\varepsilon_k}{2\ln\left(\frac{R_c}{r_w}\right)}\frac{f}{s}\int_{\frac{r_w}{R_c}}^{1}\frac{C(r_D)\cdot Y(r_D)}{r_D^2}dr_D\right)t_D \qquad (D-6)$$

From Eq. (D-6) follows that the impedance is a linear function of time (see Eq. (3)). Substitution of different order approximations (C-3), (C-5) and (C-7) into Eq. (2) results in explicit but cumbersome expressions.

References

Alvarez, A.C., Bedrikovetsky, P., Hime, G., Marchesin, D., Rodríguez, J.R., 2006a. A fast inverse solver for the filtration function for flow of water with particles in porous media. J. Inverse Probl. 22, 69–88.

Alvarez, A.C., Hime, G., Marchesin, D., Bedrikovetsky, P., The inverse problem of determining the filtration function and permeability reduction in flow of water with particles in porous media (accepted by Journal of Transport in Porous Media on 10/ 2006).

Allaga, D.A., Wu, G., Sharma, M.M., Lake, L.W., 1992. Barium and calcium sulphate precipitation and migration inside sandpacks. SPEFE. March.

Araque-Martinez, A. and Lake, L.W., 1999. A simplified approach to geochemical modelling and its effect on well impairment. SPE Paper 56678, SPE Annual Technical Conference and Exhibition, Houston, Texas, 3 6 October.

Bedrikovetsky, P.G., 1994. Mathematical Theory of Oil and Gas Recovery. Kluwer Academic Publishers, London/Boston.

Bedrikovetsky, P.G., Monteiro, R.P.S., Lopes Jr., R.P., Moraes, G.P., Carageorgos, T., Rosário, F.F., Lima, E.A., 2006a. Mathematical and laboratory modeling of reservoir sulphate scaling. In: Lakatos, I. (Ed.), Mining and Oilfield Chemistry. Akadémiai Kiadó, Budapest, Hungary.

Bedrikovetsky, P.G., Mackay, E.J., Monteiro, R.P.S., Moraes, G.P. and Rosário, F.F., 2006b. Laboratory- and field prediction of sulfate scaling damage. SPE Paper 100611, SPE International Oilfield Scale Symposium, Aberdeen, Scotland, U.K., 30 May–1 June.

Bethke, C., 1996. Geochemical Reaction Modelling. Oxford University Press. 397.

Bezerra, M.C., Rosario, F.F., Khalil, C.N., Milanez, P.V., 1996. Prevention and control in Namorado Field, Campos Basin, Brazil. NACE International Annual Conference and Exposition.

Civan, F., 2000. Reservoir Formation Damage. Fundamentals, Modeling, Assessment and Mitigation. Gulf Professional Publishing. 705.

Daher, J.S., Gomes, J.A.T., Rosário, F.F., Bezerra, M.C., Mackay, E.J., Sorbie, K.S., 2005. Evaluation of inorganic scale deposition in unconsolidated reservoir by numerical simulation. SPE Paper 95107, 7th International Symposium on Oilfield Scale, Aberdeen, UK, 11–12 May.

Daher, J.S., Gomes, J.A.T., Rosário, F.F., Bezerra, M.C., 2006. Field experience to assess efficiency of scale dissolver treatment in a subsea deep water well. SPE Paper 100653, 8th International Symposium on Oilfield Scale, Aberdeen, UK, 30 May–1 June.

Dake, L.P., 1978. Fundamental of Reservoir Engineering. Elsevier Scientific Publishing Company.

Delshad, M., Pope, G.A., 2003. Effect of dispersion on transport and precipitation of barium and sulphate in oil reservoir. SPE Paper 80253 Presented at the SPE International Symposium on Oilfield Chemistry held in Houston, Texas, USA, 5–7 February.

Dunn, K., Daniel, E., Shuler, P., et al., 1991. Mechanisms of precipitation and dissolution of barite: a morphology approach. J. Colloid Interface Sci. 214, 427–437.

Eclipse, 2001. Technical Description, Chapter 61. Well Modelling Facilities, Scale Deposition Model. Schlumberger.

Fogler, S., 1998. Chemical Reactions Engineering. Prentice Hall, New York City.

Gomes, J., Bezerra, M.C., Daher, J.S., Rosario, F.F., 2002. The impact of mineral scale formation on deep water fields: a Campos Basin overview. SPE Oilfield Scaling Symposium, Aberdeen, UK, 30–31 January.

Goulding, P.S., 1987. Formation damage arising from barium sulphate scale precipitation. Ph.D Thesis, Heriot-Watt University, Scotland, UK.

Lopes, R.P.J., 2002. Barium sulphate kinetics of precipitation in porous media: mathematical and laboratory modelling, in Portuguese. MSc. Thesis, North Fluminense State University, Macaé, Rio de Janeiro.

Mackay, E.J, Jordan, M.M., Torabi, F., 2002. Predicting brine mixing deep within the reservoir, and the impact on scale control in marginal and deepwater developments. SPE Paper 73779. SPE International Symposium and Exhibition on Formation Damage Control, Lafayette, LA, 20–21 February.

Mackay, E.J., 2002. Modelling of in-situ scale deposition: the impact of reservoir and well geometries and kinetics reaction rates. SPE Paper 74683, Oilfield Scaling Symposium, Aberdeen, UK, 30–31 January.

Nancollas, G., Liu, T., 1975. Crystal Growth and Dissolution of Barium Sulphate. SPE Paper 5300 Presented at 1975 SPE/AIME Oilfield Chemistry Symposium, Dallas, January.

Nikolaevskii, V.N., 1990. Mechanics of Porous and Fractured Media. World Scientific Publishing Co., Singapore.

Oddo, J.E. and Tomson, M.B., 1994. Why scale forms and how to predict it. SPEPF, 47–54, February.

Oren, P.E., Bakke, S., 2002. Process based reconstruction of sandstones and prediction of transport properties. Transport in Porous Media, V. 46, 311–343.

Pang, S., Sharma, M.M., 1994. A model for predicting injectivity decline in water injection wells. SPE Paper 28489, SPE 69th Annual Technical Conference and Exhibition, New Orleans, LA, September 25 28.

Philips, O.M., 1991. Flow and Reactions in Porous Media. Cambridge University Press, Cambridge, UK.

Read, P.A., Ringen, J.K., 1982. The use of laboratory tests to evaluate scaling problems—during water injection. SPE Paper 10593, SPE Sixth International Symposium on Oilfield and Geothermal Chemistry, Dallas, Texas, 25–27, January.

Rocha, A., Frydman, M., Fontoura, S., Rosario, F.F., Bezerra, M.C., 2001. Numerical modelling of salt precipitation during produced water reinjection. SPE Paper 68336 SPE Third International Symposium on Oilfield Scale, Aberdeen, UK, 30 31 January.

Rosario, F.F., Bezerra, M.C., 2001. Scale potential of a deep water field — water characterisation and scaling assessment. SPE Paper 68332, SPE Third International Symposium on Oilfield Scaling, Aberdeen, UK, 30 31 January.

STARS, 2003. Advanced Process and Thermal Reservoir Simulator, User's Guide. CMG, Computer Modelling Group Ltd, Calgary, Canada.

Sorbie, K.S., Mackay, E.J., 2000. Mixing of injected, connate and aquifer brines in waterflooding and its relevance to oilfield scaling. J. Petrol. Sci. Eng. 27, 85 106.

Todd, A.C. and Yuan, M.D., 1992. Barium and strontium sulphate solid-solution scale formation at elevated temperatures. SPEPE, 85–92, February.

Watt, R.M.S., Sorbie, K.S., Todd, A.C., 1992. Kinetics of $BaSO_4$ crystal growth and effect in formation damage. SPE Paper 23814 SPE International Symposium on Formation Damage Control, Lafayette, Louisiana, 26–27 February.

Woods, A.W., Parker, G., 2003. Barium sulphate precipitation in porous rock through dispersive mixing. SPE Paper 80401 SPE 5th International Symposium on Oilfield Scale, Aberdeen, UK, 29–30 January.

Yuan, M., 1989. Prediction of sulphate scaling tendency and investigation of barium and strontium sulphate solid solution scale formation. Ph.D. Thesis, Heriot-Watt University, Scotland, UK.

Glossary

c_{Ba}: Ba^{2+} molar concentration in aqueous solution, nmol/L^3, gmol/L
c_{SO_4}: SO_4^{2-} molar concentration in aqueous solution, nmol/L^3, gmol/L
C: dimensionless Ba^{2+} concentration
D: dispersion coefficient, L^2/t, m^2/s
h: thickness, L, m
PI: productivity index, L^4t/m, $m^3/(s \times Pa)$
J: dimensionless impedance
k^0: initial permeability, L^2, mD
K_a: chemical reaction rate constant, $(M\ s)^{-1}$ (2nd order reaction)
m: slope of the impedance straight line
M: molar unit for concentration equals gmol/L (same as kgmol/m^3)
M_{BaSO_4}: molecular weight for barium sulphate equals 0.23339 kg/mol
p: pressure, m/Lt^2, Pa
p_D: dimensionless pressure
Q: total rate, L^3/t, m^3/s
r: radial co-ordinate, L, m
r_D: dimensionless coordinate
R_c: contour radius, L, m
r_w: well radius, L, m
S: dimensionless $BaSO_4$ concentration
t: time, t, s
t_D: dimensionless time
U: flow velocity, L/t, m/s
V: concentration difference
Y: dimensionless SO_4^{2-} concentration

Greek letters

α: ratio between injected concentrations of Ba^{2+} and SO_4^{2-}
α_D: dispersion coefficient, L, m
β: formation damage coefficient
ε_D: dimensionless diffusive (Schmidt) number
ε_k: dimensionless chemical kinetics number
ϕ: Porosity
λ: kinetic coefficient, $(M\ m)^{-1}$ (2nd order reaction)
μ: viscosity, m/Lt, kg/(m × s)
ρ_{BaSO_4}: density of the barite, 4193.9 kg/m^3
σ: $BaSO_4$ molar concentration in solid deposit